DISSERTATIONES CHIMICAE UNIVERSITATIS TARTUENSIS
87

DISSERTATIONES CHIMICAE UNIVERSITATIS TARTUENSIS
87

MARKO LÄTT

Carbide derived microporous carbon and electrical double layer capacitors

TARTU UNIVERSITY
PRESS

Institute of Chemistry, Faculty of Science and Technology, University of Tartu, Estonia

Dissertation is accepted for the commencement of the Degree of Doctor of Philosophy in Physical and Analytical Chemistry on June 17th, 2009 by the Doctoral Committee of the Institute of Chemistry, University of Tartu.

Supervisors: Professor, Dr. Enn Lust, University of Tartu, Estonia
Dr. Alar Jänes, University of Tartu, Estonia

Opponents: Dr. Kyösty Kontturi, Helsinki University of Technology, Finland

Commencement: August 28th 2009 at 14:00, 18 Ülikooli St., room 204

Publication of this dissertation is granted by University of Tartu

ISSN 1406–0299
ISBN 978–9949–19–169–7 (trükis)
ISBN 978–9949–19–170–3 (pdf)

Autoriõigus Marko Lätt, 2009

Tartu Ülikooli Kirjastus
www.tyk.ee
Tellimus nr. 273

CONTENTS

LIST OF ORIGINAL PUBLICATIONS

I. Leis, J., Arulepp, M., **Lätt, M.,** Kuura, H., Kuura, A., "Method for manufacturing the nanoporous SkeletonC material", *United States Patent Application No.* US 0251565 A1, **2006.**

II. Leis, J., Arulepp, M., **Lätt**, **M.,** Kuura, H., "Method of making the porous carbon material and porous carbon materials produced by the method", *United States Patent Application No.* 0117094 A1, **2009**.

III. Leis, J., Arulepp, M., Kuura, A., **Lätt, M.,** Lust, E., "Electrical double-layer characteristics of novel carbide-derived carbon materials", *Carbon* **2006**, 44(11), 2122–2129.

IV. Arulepp, M., Leis, J., **Lätt, M**., Miller, F., Rumma, K., Lust, E., Burke, A.F., "The advanced carbide-derived carbon based supercapacitor", *J Power Sources* **2006**, 162(2), 1460–1466.

V. **Lätt, M.,** Käärik, M., Permann, L., Kuura, H., Arulepp, M., Leis, J., "A structural influence on the electrical double-layer characteristics of Al_4C_3-derived carbon", *J Sol State Electrochem.* **2008**, doi:10.1007/s10008-008-0659-3.

AUTHOR'S CONTRIBUTION

The author performed the microporous carbon material synthesis, contributed to the design and construction of the reactors and synthesis equipment and performed the experiments on the process cycle stages (I, II, III, IV, V). The author contributed to the construction of the experimental EDLC devices (III, IV, V), the manufacture of microporous carbon electrodes (III, IV, V) and to the electorchemical experiments and their interpretation (IV, V).

INTRODUCTION

Carbon, the sixth most abundant element in the universe has been known since ancient times. It is found in abundance in the sun, stars, comets, and atmospheres of most planets. The ability of carbon to bond with itself and other elements in a seemingly endless array of varied combinations forms the basis of all known life and that in turn gave rise to the vast and sprawling scientific discipline that is now known as the modern organic chemistry. In 1722, René A. F. de Réaumur demonstrated that iron was transformed into steel through the absorption of some substance, now known to be carbon. In 1772, Antoine Lavoisier demonstrated that diamonds are in fact a form of carbon, when he burned samples of carbon and diamond and revealed that neither produced any water and that both released the same amount of carbon dioxide per gram. Carl Wilhelm Scheele showed that graphite, which had been thought of as a form of lead, was instead a type of carbon. In the year 1786, the French scientists Gaspard Monge, Claude Louis Berthollet and C. A. Vandermonde showed that this substance was carbon. In their publication they proposed the name *carbone* for this element. Antoine Lavoisier listed carbon as an element in his textbook published in the year 1789.

This research is dedicated to the optimization of the production process of carbide derived carbon (CDC) and to the application of these materials in the field of electrical double layer energy storage devices (EDLC) also known as supercapacitors. The electrochemical properties of carbonaceous materials in capacitor applications have been extensively studied for a long time, but still there are many problems that are in need of clarification and solving [1]. The structural and pore size related properties of the carbon materials used in the above mentioned application have the utmost importance, as they determine the behavior and performance of the electrical double layer capacitor [1–3]. In theory the capacitance of an EDLC device should be in direct correspondence with the specific surface area of the carbon material used as the electrode material [1]. However, in reality, the relationship is more complicated and also depends on the pore size related properties of the carbon material used. Controlling and shaping these properties is done by choosing the optimal conditions in the carbon production stage. Finding a way to define these optimal conditions, as good as possible, is the goal of the current research.

The overall reaction of carbide derived carbon production process can be described as follows:

$$MC_x + y/2Cl_2 \rightarrow MCl_y + xC \quad (1)$$

where M describes the metal or metalloid forming the carbide and y,x are the corresponding stoichiometric coefficients.

Depending on the variable reaction conditions, the carbide used and the carbide's structural properties, it is possible to produce a wide variety of carbon structures, ranging from totally amorphous carbon with fine tuned pore size

parameters [1–4,V] (for electrical double layer capacitors), to nanotube like barrels and graphitic formations (for possible intercalation of lithium ions or novel electronic solutions) [4–8]. The appeal of this particular method is the fact that it allows for a reasonably priced industrial scale production of nano-structured carbon to become real, with the implementation of a process cycle and some improvements on the general setup. Although the chlorination process can be used to create a wide range of carbon structures with controllable parameters, the amorphous carbon, in light of EDLC application, is getting most of the attention. In particular the carbon derived from titanium carbide. With a suitable pore size range in the derived amorphous carbon, reasonable availability and wide-spread application in current industrial processes, it creates a prime candidate for the raw material of the chlorination process. Due to the wide use of titanium carbide, titanium oxide and titanium tetrachloride, it is possible to realize a process cycle utilizing all of the waste and sideproducts of the carbide derived carbon production, thus minimizing costs and producing a superior carbon for the EDLC application.

1. METHODS USED IN CHARACTERIZATION OF NANOPOROUS AMORPHOUS CARBON

The structure of carbon materials can be determined by a variety of methods based on physico-chemical or quantum mechanics related properties of the material [1,9]. As this work concentrates on the material being used in an EDLC application, so do the methods involved concentrate on reflecting the physical and porosity related parameters of the material. There is a wide variety of methods that can be used to determine the porosity related parameters of a porous material and in case of carbon, most of the methods for determining a solid materials' porosity can be applied. Following the definitions of IUPAC, the carbon materials can be divided into macro- (>500Å), meso- (20–500Å) and microporous (<20Å) materials according to their pore size[10]. Microporous materials can be further divided into materials with narrow (<7Å) and wide (7–20Å) micropores[11,12]. A detailed interpretation of the pore size structure in terms of pore size distribution is vital for predicting the performance of microporous carbon materials in many applications as well as for the tailoring of new porous materials.

1.1 Dynamic molecular probe

Adsorption dynamics measurement of solvent vapors is probably the simplest way to determine the porosity of a material. The experiment is usually carried out in room temperature and normal pressure using a computer controlled weighing system to register the changes of the sample mass in time. The changes of the sample mass are registered until a constant weight has been achieved by the equilibrium of the sorption/desorption rates. The volume of micropores is then calculated according to the equation:

$$W_s=(m_2-m_1)/m_1 d_{solvent} \quad (2)$$

where m_1 and m_2 are the initial and final mass of the sample, respectively and $d_{solvent}$ is the density of the solvent (typically benzene, in case of a carbon sample) used at the current room temperature during the experiment.

1.2 Low temperature nitrogen sorption

Adsorption is usually described through adsorption isotherms, reflecting the amount of adsorbate on the adsorbent as a function of its pressure (in case of a gas) or concentration (in case of a liquid) at constant temperature. The quantity adsorbed, is usually normalized by the mass of the adsorbent, to allow for comparison of different materials [8,11].

The first mathematical fit to an isotherm was published by Freundlich and Küster in 1894 and it is a purely empirical formula for gaseous adsorbates [12–14]:

$$\frac{x}{m} = kP^{\frac{1}{n}} \tag{3}$$

where x is the quantity adsorbed, m is the mass of the adsorbent, P is the pressure of adsorbate and k and n are empirical constants for each adsorbent-adsorbate pair at a given temperature. The function has an asymptotic maximum as pressure increases without boundary. As the temperature increases, the constants k and n change to reflect the empirical observation that the quantity adsorbed rises more slowly and higher pressures are required to saturate the surface.

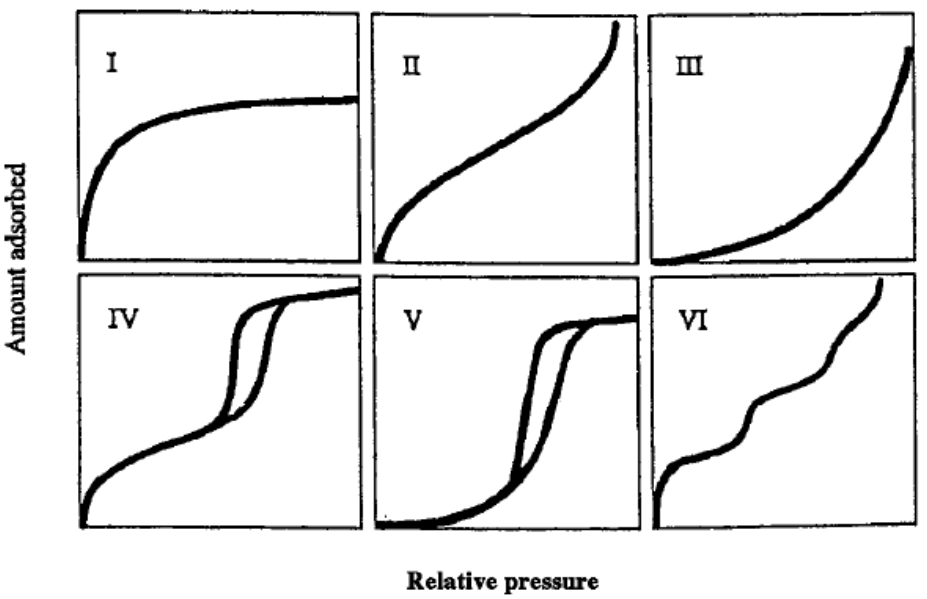

Figure 1. IUPAC classification of adsorption-desorption isotherms.

There are six principal types of adsorption isotherms as illustrated in Figure 1. Type I is the characterisitic reversible isotherm of microporous materials saturating at low relative pressures. Type II isotherm is typical for nonporous or mesoporous materials, representing unrestricted monolayer/multilayer adsorption. The reversible type III isotherm is not very often encountered and it is associated with adsorption on surfaces with low adsorption potential (e.g. organic polymers). Type IV isotherms resemble type II, but a hysteresis loop exists. Occurrence of hysteresis is associated with capillary condensation in

mesopores and the limiting effect of that on gas uptake at higher relative pressures. This type of isotherm is characteristic of mesoporous materials. Type V isotherm is uncommon, but encountered in cases where adsorbent-adsorbate interactions are exceptionally weak compared to adsorbate-adsorbate interactions (e.g. water vapour adsorption on microporous carbon). Type VI isotherm represents stepwise adsorption on multilayers of nonporous materials. The step height represents the monolayer adsorption capacity [8, 13–15].

To enable the comparison of different materials a method for quantitative isotherm interpretation is needed. However, the interpretation of adsorption desorption isotherms is not straightforward [14]. Especially the adsorption in micropores is difficult to describe adequately. The interpretation of adsorption isotherms is carried out by applying mathematical models to the isotherm data. There exist several models for that purpose, the most widely used being the Langmuir, BET (Brunauer- Emmet- Teller), D-R (Dubinin –Radushkevich) and DFT (Density Functional Theory) [16–18].

The low temperature nitrogen sorption/desorption measurements in the current study were carried out at the boiling point of nitrogen (–196°C). The specific surface areas of the materials were calculated according to BET and Langmuir theories up to nitrogen relative pressure (p/p_0= 0.2). The total pore volume V_{tot} can be calculated from the volume of nitrogen absorbed at near saturation pressure (p/p_0 =0.95). The volume of micropores V_m can be derived from the nitrogen sorption isotherm.

1.3 X-ray diffraction spectrometry

X-ray powder diffraction technique is a non-destructive analysis method that reveals information about the crystallographic structure, chemical composition, and physical properties of materials and thin films under study. The technique is based on observing the scattered intensity of an X-ray beam hitting a sample as a function of incident and scattered angle, polarization, and wavelength or energy [19].

When the scattered radiation is collected on a flat plate detector, the rotational averaging leads to smooth diffraction rings around the beam axis, rather than the discrete Laue spots as observed for single crystal materials' diffraction. The angle between the beam axis and the ring is called the scattering angle and in X-ray crystallography always denoted as 2θ. In accordance with Bragg's law, each ring corresponds to a particular reciprocal lattice vector *G* in the sample crystal. This leads to the definition of the scattering vector as [20,21]:

$$G = q = 2\,k\,\sin(\theta) = 4\,\pi\,\sin(\theta)\,/\,\lambda. \quad (4)$$

Powder diffraction data are usually presented as a diffractogram, in which the diffracted intensity is shown as function either of the scattering angle 2θ or as a

function of the scattering vector q. The latter variable has the advantage that the diffractogram no longer depends on the value of the wavelength λ. The advent of synchrotron sources has widened the choice of wavelength considerably. To facilitate comparability of data obtained with different wavelengths, the use of q is therefore recommended and gaining acceptability [20,21].

The most widespread use of X-ray powder diffraction is the identification and characterization of crystalline solids, each of which produces a distinctive and unique diffraction pattern. Both, the positions of the peaks (corresponding to the spacings in the cristal lattice) and the relative intensity of the lines are indicative of a particular phase and material, providing a spectral fingerprint for comparison. A multi-phase mixture, *e.g.* a polycristalline soil sample, will show several patterns superposed, allowing for the determination of relative concentrations.

In contrast to a crystalline pattern, consisting of a series of sharp peaks, amorphous materials (amorphous carbon), produce a broad background signal. In carbon materials consisting of graphite-like structural fragments, two 00*l* and two *hk*0 maxima appear in the XRD spectra, as seen in Figure 2, in good agreement with [21,22].

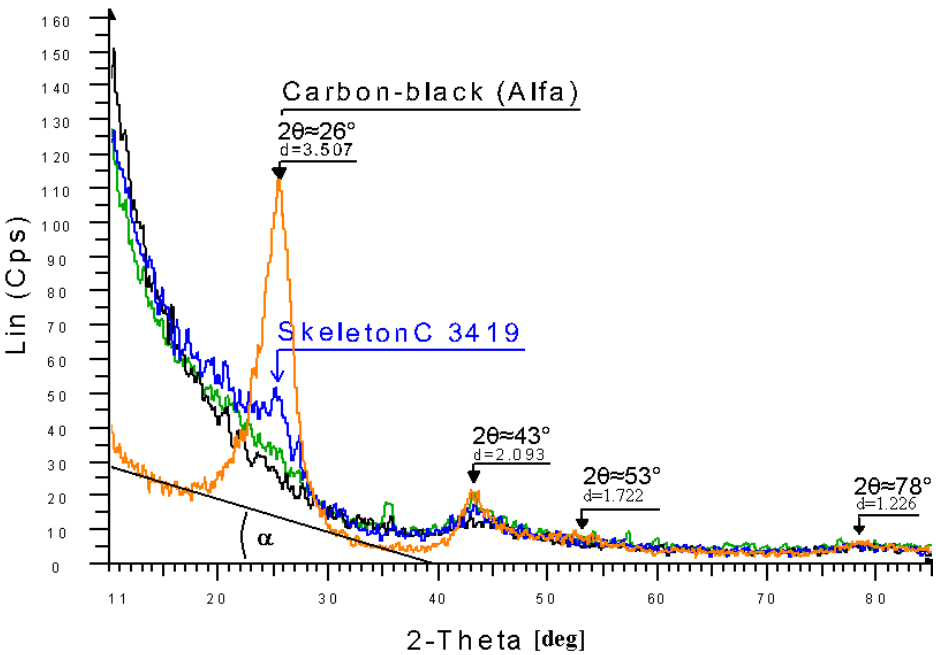

Figure 2. Powder XRD spectra for carbon samples with different degrees of graphitisation.

The 002 and 004 peaks at 2θ≈26° and 2θ≈53° correspond to parallel graphene layers. The 100 and 110 peaks at 2θ≈43° and 2θ≈78° characterise the 2D in

plane symmetry along the grpahene layers [20,22]. The 00*l* peaks are almost absent in carbon samples with high specific surface area and amorphous structure. A second important characteristic of the XRD spectra is the angle α between the background line under the 002 reflection and the 2θ axis. It has been shown that this angle is proportional to the relative amount of amorphous material in the sample and can therefore be used as an estimate to the degree of disorder in the carbon material [19–24].

2. SYNTHESIS OF NANOPOROUS AMORPHOUS CARBON BY CHLORINATION METHOD

During the course of the current study several samples of the amorphous carbon materials were produced, utilizing three different chlorination reactor types: stationary bed reactor, rotary bed reactor and fluidized bed reactor. All the reactors have a quartz core tube that can withstand the high temperature and corrosive environment of the reagents [I-V]. The general reaction is carried out in conditions where the formed byproduct (the metalloid or metal chloride) is in a gaseous form and can be carried out of the reaction zone by excess gases. After exiting the reactor, the byproduct can be neutralized with a suitable reagent or collected for further implementation in the process cycle.

Stationary bed reactor is composed of a quartz tube into which a carrier with the carbide sample is loaded. This reactor type is predominantly used for the chlorination of small pilot batches for quick testing of carbon materials under study. The reactor is not efficient, nor does it produce uniform conditions along the movement direction of the reagent gas. This manifests itself in the varied properties of the resulting CDC, when sampled along the gas movement direction.

Figure 3. Experimental stationary bed reactor.

Rotary bed reactor is a more complex device, consisting of two quartz tubes with different diameters. The smaller tube is rotated inside the bigger one on graphite bearings, creating a rotary bed that can handle a much bigger amount of carbide, compared to the stationary bed reactor type and due to the mixing effect, produces uniform conditions inside the reaction zone. The reactor type is suitable for the batch chlorination of bigger amounts of carbide with a fine particle size (around 3μm). Efficiency is mediocre, remaining between 75–85% of the theoretical yield for the reaction.

Figure 4. Experimental rotary bed reactor.

Fluidized bed reactor is by far the most efficient and from an industrial viewpoint the most rational tool for carrying out this type of chlorination reaction. Depending on reactor construction and reaction conditions, it can handle from two to three times more precursor carbide in half the reaction time and with nearly 100% efficient chlorine consumption, compared to rotary bed reactor with the same reaction zone capacity. Unfortunately the fluidized bed reactor can not handle the carbide with a fine enough particle size to directly qualify for EDLC electrode production. At such particle sizes the carbon materials' loss through mass transport would approach 100%. This means that an agglomerate or a much coarser carbide in need of post chlorination milling will have to be used as a starting material.

Figure 5. Experimental fluidized bed reactor.

After the chlorination step, the resulting carbon material needs further attention to remove the adsorbed chlorine and other functional groups from the active surface of the carbon by hydrogen treatment, and if there should be a need for it, receive additional aftertreatment (e.g. H_2O vapour etching) [23,24]. The waste chlorides create another complication, as they have to be disposed of in a safe manner. Both of these steps require additional effort. But both of these steps can be eliminated by the use of on site oxidation via TiO_2 during the chlorination process and by implementing the process cycle that allows for the reuse of all waste products from the chlorination stage [I-III].

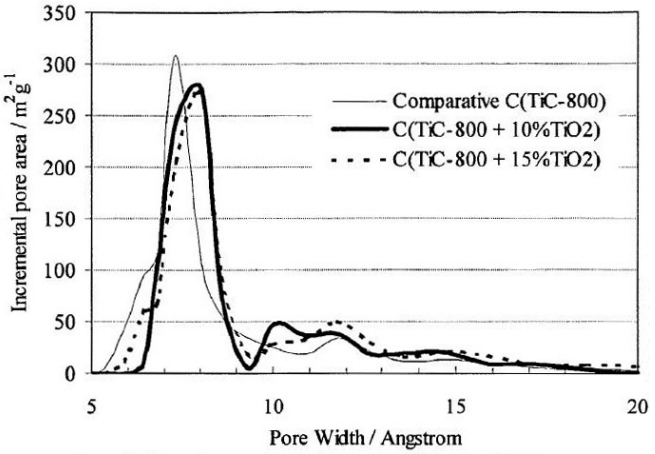

Figure 6. DFT pore size distribution of different SkeletonC powders derived from fine-grain TiC (H.C. Stack) without additives (solid line); with 10%wt. TiO_2 additive in TiC (bold line) and with 15%wt. TiO_2 additive in TiC (dotted line) at the chlorination stage.

It is known that the microporous carbon derived from TiC below 900°C is predominantly amorphous and does not contain long range structures according to X-ray diffraction and high-resolution transmission electron microscopy studies [23,24]. Such carbon possesses BET surface area up to 1400 m^2 per gram and is almost completely microporous with a peak pore size of ~7 Å. In fact, the very small micropores, below 6–7 Å, are mostly inaccessible to the electrolyte ions [8,25,26]. The impact of pores below 6Å can be reduced by different oxidative post-modification treatment methods [II, III].

One example of these methods is the *in situ* oxidation of CDC with TiO_2, which enables to minimize the formation of such inaccessible micropores during chlorination of the carbide [II]. The method implements the known carbothermal reduction of TiO_2 in chlorine atmosphere:

$$2C + TiO_2 + 2Cl_2 \rightarrow TiCl_4 + 2CO \quad (5)$$

The essence of the method is the fact that TiO_2 oxidizes the predetermined small part of the carbon created during carbide etching with the chlorine. The process, thereby, is well controlled by the amount of TiO_2 in the reaction medium.

3. PROCESS CYCLE

In the current study the focus has been cast on researching the below pictured process cycle in Figure 7 and the different stages thereof, to establish some understanding on how the different parameters involved in this cycle interact on each other. This knowledge is invaluable in the practical implementation of the process cycle at hand. The cycle itself contains four separate stages that make it possible to reuse most of the excess reagents and waste products formed during the production of carbide derived carbon. Stage C and stage D, the synthesis of titanium carbide and the synthesis of carbide derived carbon from the resultant carbide respectively, have been thoroughly researched during the course of this work, as they hold the key aspects to producing superior CDC materials for EDLC application.

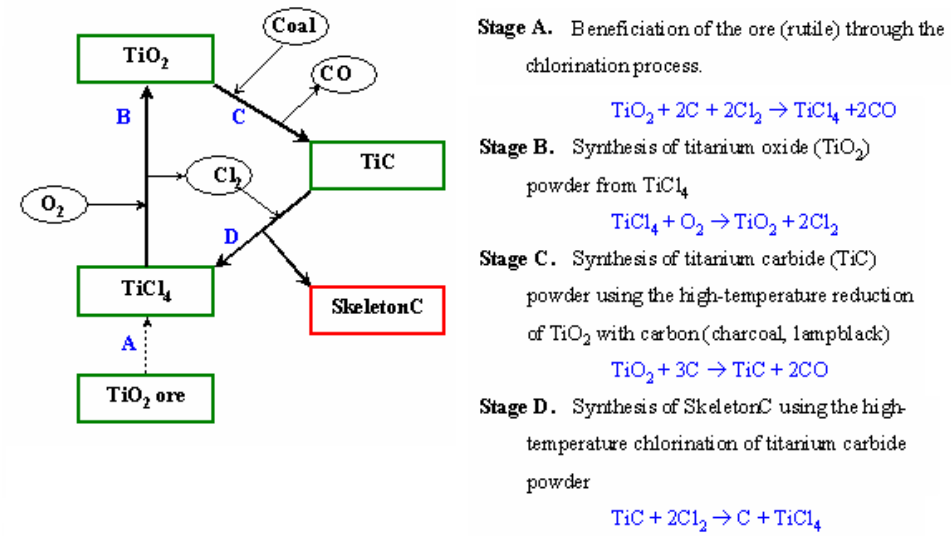

Figure 7. Process cycle for the production of CDC material from TiC precursor.

3.1 Carbide synthesis stage

A number of carbide synthesis reactions were carried out by reacting titanium dioxide powder (Aldrich, Alfa Aesar) with carbon (lampblack Alfa Aesar) under high temperature (1200–1600°C) in an inert atmosphere of argon gas (AGA 2.1). A graphite core high temperature reactor was used to create the required conditions. The precursor mixture of TiO_2 and lampblack C was prepared by mechanically mixing the ingredients with the aid of n-propanol as a wetting agent. After desiccation the mixture was loaded into a graphite capsule, placed into the reactor and held at the desired temperature for one hour to complete the reaction. The resulting carbide samples were characterized by X-

ray diffraction analysis to reveal any trends in the change of crystalline structure vs. reaction temperature and precursor mixture.

The overall reaction for the carbide synthesis stage can be described as a sum of the following:

$$TiO_2 + 3C \rightarrow TiC + 2CO \quad (6)$$
$$TiO_2 + 2C \rightarrow TiC + CO_2 \quad (7)$$

Experimental data suggests that both of the reactions compete with each other with the balance depending on reactor temperature.

Figure 8. Experimental high temperature reactor and graphite capsule for carbide synthesis.

3.2 Cristalline stoichiometry shift with varied synthesis parameters

According to X-ray diffraction data, it was observed, that with the rise of reaction temperature from 1400°C to 1600°C the crystalline stoichiometry of the formed titanium carbide shifted towards the normal value of 0.85 (TiC_x with x=0.85). At lower reaction temperatures the formed crystalline phase was less saturated by carbon and at higher temperatures it was more saturated, approaching the boundary of 0.85 at 1600°C [I].

The carbide formation reaction goes through several inermediates at lower temperatures, in the range of 1200°C to 1350°C, as can be observed in the spectra displayed in Figure 9. At 1200°C the intermediate can be identified as being partially Ti_2O_3, as can be observed from the spectra in Figure 10. At higher temperatures around 1300°C the intermediate becomes unidentifiable by the comparison of standard X-ray diffraction spectra [I].

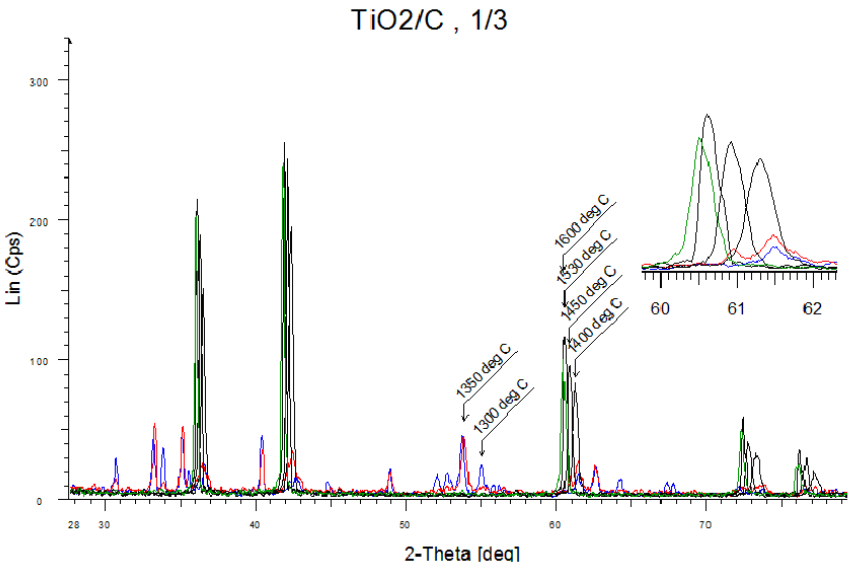

Figure 9. The shift in crystalline stoichiometry of TiC at varied synthesis temperature.

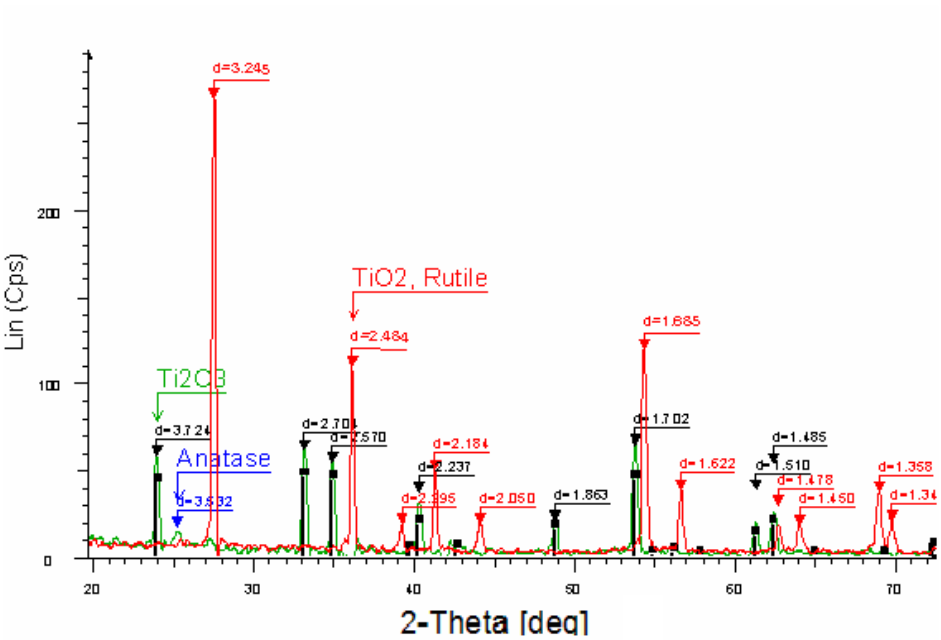

Figure 10. The intermediate of the carbide formation reaction at 1200°C.

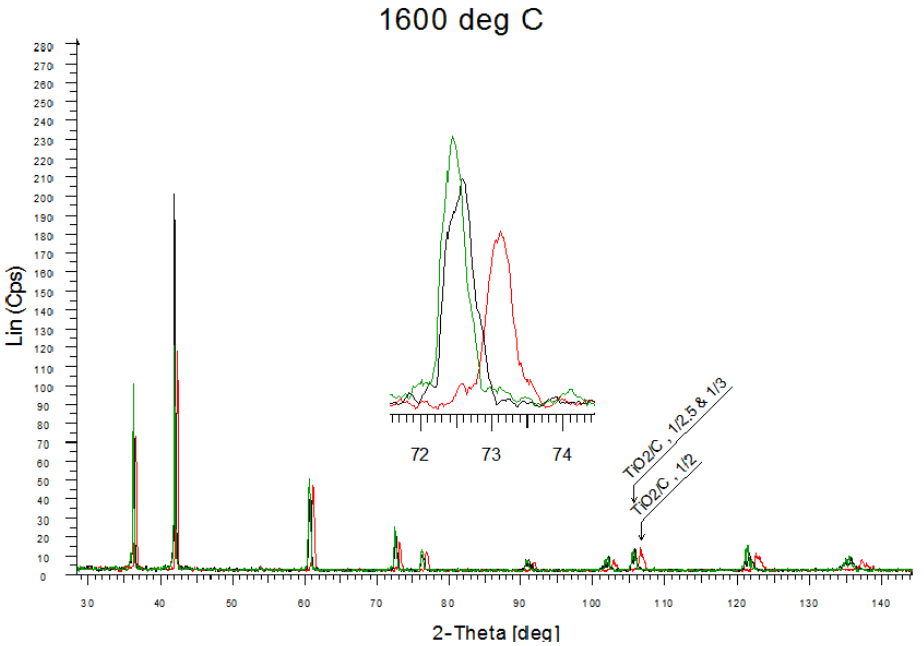

Figure 11. The shift in crystalline stoichiometry of TiC at varied precursor mixtures.

By varying the composition of the precursor mixture TiO_2 / C as follows: (1/2, 1/2.5, 1.2.7, 1/3, 1/3.3), a similar stoichiometry shift was observed at 1600°C as can be seen from the spectra in Figure 11. The more carbon a precursor mixture contains, the richer in carbon was the resulting carbide phase. At a certain point the excess carbon remains unreacted and becomes a ballast in the carbide, as will be revealed by chlorinating the oversaturated carbide samples and evaluating the resulting CDC.

3.3 Amorphous microporous carbon synthesis stage

A number of microporous carbon materials (SkeletonC CDC) were synthesized from the carbide samples created in the above mentioned experiment series, by chlorination in a stationary bed reactor at 800°C. The resulting materials were characterized by X-ray diffraction analysis, dynamic molecular probe method and the low temperature nitrogen sorption method. The carbon materials produced were amorphous in structure and depending on the carbide precursor had a specific surface area, ranging from 1000m^2/g to 1920 m^2/g [I-III]. The general reaction is described as:

$$TiC+2Cl_2 \rightarrow C + TiCl_4 \quad (8)$$

Table 1. Characteristics of the TiC precursors and the respectively derived carbon materials.

Carbide synthesis stage		Amorphous carbon synthesis stage			
Carbide precursor molar ratio(TiO_2/C)	$T_{synthTiC}$ [°C]	T_{synthC} [°C]	Carbon yield [%]	W_s	S_{BET} [m^2/g]
½	1600	800	–	–	–
1/2.5	1600	800	53	1.54	1920
1/2.7	1600	800	66	0.95	1754
1/2.7	1600	800	66	0.88	1579
1/3	1600	800	93	0.55	1229
1/3	1600	800	99	0.4	1100
1/3.3	1600	800	120	0.53	1079
1/3.3	1600	800	114	0.4	1016

Carbide precursor molar ratio – describes the molar ratio of TiO_2 and carbon black used in the TiC precursor mixture
$T_{synthTiC}$ – the synthesis temperature in [°C] of the carbide production phase
T_{synthC} – the chlorination temperature in [°C] of the CDC production stage
Carbon yield – the chlorination yield in [%] of the theoretical value
W_s – the porosity according to molecular probe analysis (benzene vapour adsorption)
S_{BET} – the specific surface area in [m^2/g] according to BET theory

Table 1. illustrates the porosity related characteristics of the microporous carbon materials synthesized from respective carbides through different precursor mixtures.

The carbide from the precursor with a molar ratio of 1/2 was unable to yield any carbon during in the chlorination process. The formed carbon supposedly has a very low density and is therefore extremely prone to being etched by excess chlorine and titanium tetrachloride during the process. This leads to the complete destruction of the sample. As the molar ratio of the precursor mixture reaches 1/3 a significant drop in the micropore volume and in the specific surface area S_{BET} is observed. This is due to the unreacted carbon black, which remains as a ballast in the carbon sample after chlorination and significantly lowers the values of S_{BET} for material synthesized. This fact is also confirmed by X-ray diffraction analysis of the carbon materials, as can be observed on the spectra in Figure 12. With carbon materials derived from carbides originating from precursor mixtures with a molar ratio equal to or less of than 1/3, the distinct 002 peak at $2\theta \approx 26°$ is observed, as a result of the unreacted carbon black in the sample.

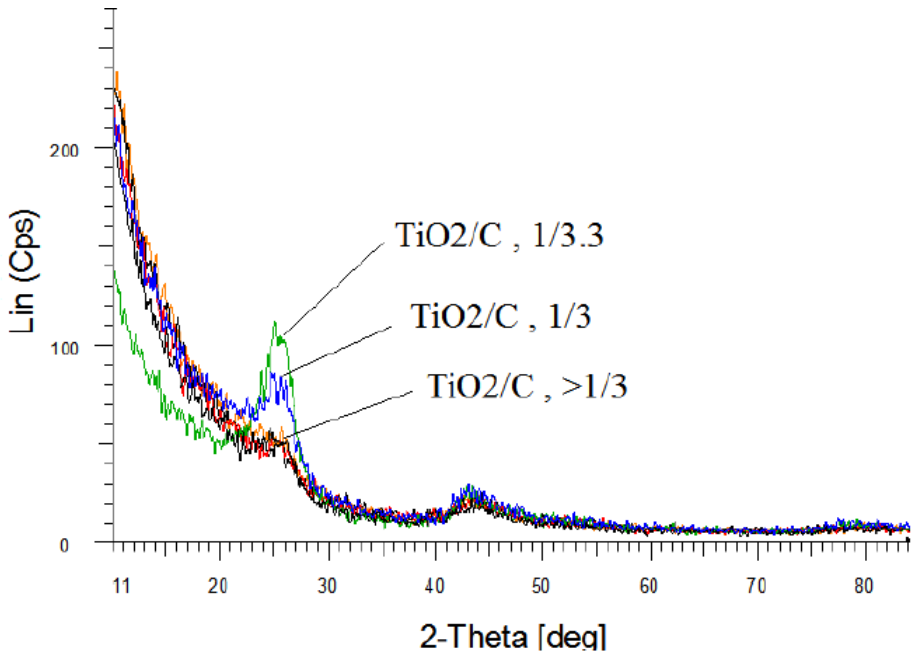

Figure 12. The X-ray diffraction spectra of carbon materials derived from carbides with different precursor mixtures.

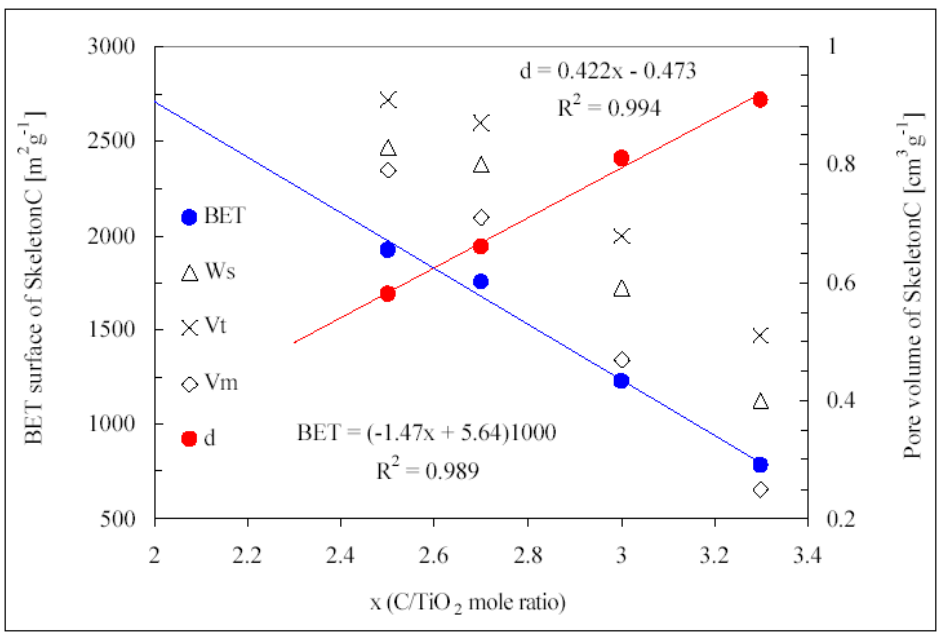

Figure 13. Relation of different synthesis parameters on the characteristics of the resulting CDC.

Figure 13 clearly illustrates the effects of different synthesis parameters incorporated in carbide and carbon synthesis stages on the resulting microporous carbon material. The ideal region for producing amorphous carbon designated for EDLC application lies near the precursor mixture molar ratio of 1/2.7 and near 1600°C of reaction temperature for the carbide synthesis stage. This combination guarantees a high specific surface area for the CDC material accompanied by a reasonable chlorination stage yield and a satisfactory carbon material bulk density. As we drift away from this range in either direction the quality of the final carbon material tends to suffer, with recpect to the characteristics desirable for the EDLC application. If a carbide synthesis precursor mixture's carbon content (TiO_2/C) remarkably exceeds 1/2.7, a portion of the carbon remains unreacted, forming an inert ballast mass in the CDC, raising the carbon phase density and lowering the porosity and specific surface area. If the carbon content of a carbide synthesis precursor mixture drifts to a lower value than the 1/2.7, we create a lack of carbon in the TiC crystalline structure, resulting in a CDC with remarkably lower density and chlorination yield, yet with pronounced specific surface area and porosity values.

4. CARBIDE DERIVED CARBON IN EDLC APPLICATION

The excellent adsorbing properties of carbide-derived carbon were known already in the middle of last century [1], however, the unique microporous structure, narrow pore size distribution and possibility to fine-tune the pore size, were confirmed only recently [7,8,27–29]. Wide variability of the nanostructure and pore size distribution of CDC materials is practically achieved by varying the precursor carbide and thermal conditions of extracting the carbide forming element from crystal lattice. CDC is suggested as a suitable material in fuel cells [30] and selective adsorption processes, e.g. desalination of seawater, extraction/ purification of noble gases [31], hydrogen storage [5] etc. Another rapidly developing application field based on the adsorption behavior of porous carbon is the electrochemical energy storing devices, so-called super- or ultracapacitors [32]. Many types of CDC are tested in supercapacitors, the most promising among them seems to be the carbon derived from titanium carbide [7,8,26].

The carbide-derived SkeletonC carbon was made from fine-grain titanium carbide in the stationary bed reactor. The detailed description of making the samples and carbonaceous electrodes is described elsewhere [III,IV].

The so called "1 Farad" test-cells of EDLCs were assembled from a pair of carbon electrode discs separated with an ion-permeable cellulose based separator paper from Codashi Nippon. The visible surface area of electrodes was 2.27 cm^2.

The electrolyte used in this study was 1.2 M triethylmethylammonium tetrafluoroborate (TEMA, Stella) in anhydrous acetonitrile (AN, Riedel-de Haën, $H_2O < 0.003$ %). The TEMA salt was selected because of the use of highly microporous carbon materials, which according to the former studies, prefer the smaller Et_3MeN^+ cations, but not the Et_4N^+ ions commonly used in non-aqueous supercapacitors [33,34].

Before evaluation, the EDLC test-cells were kept at +60°C during 48 hours. Thereafter continuous cycling between 2.5 V and 1.25 V with the current $I = 100$ mA was carried out, prior to performing further electrochemical studies [35].

Table 2. Synthesis conditions and precursors of carbon material samples.

SkeletonC	Precursor	Chlorination Temperature [°C]	TiO_2 *in situ* [%]	H_2O activation [°C]
1	TiC	700	10	–
2	TiC	800	10	–
3	TiC	900	10	–
4	TiC	800	–	–
5	TiC	800	–	900
6	Coconut char*	–	–	–

*Activated carbon from coconut char (Toyota Corp.)

Table 3. Pore structure characteristics of carbon material samples.

SkeletonC	S_{BET} $[m^2g^{-1}]$	S_L $[m^2g^{-1}]$	V_P $[cm^3g^{-1}]$	V_{MP} $[cm^3g^{-1}]$	$V_{P<11Å}$ $[cm^3g^{-1}]$	$V_{P>11Å}$ $[cm^3g^{-1}]$	W_s $[cm^3g^{-1}]$
1	1453	1847	0.69	0.61	0.35	0.34	0.72
2	1588	2019	0.76	0.65	0.37	0.39	0.71
3	1841	2367	0.93	0.72	0.20	0.73	0.92
4	1348	1692	0.67	0.55	0.37	0.30	0.59
5	1451	1822	0.69	0.60	0.40	0.29	0.64
6	1898	2473	0.98	0.76	0.07	0.91	0.90

S_{BET} – the specific surface area in $[m^2/g]$ calculated according to BET theory
S_L – the specific surface area in $[m^2/g]$ calculated according to Langmuir theory
V_P – total volume of pores
V_{MP} – volume of micropores
$V_{P<11Å}$ – volume of pores with an average diameter of less than 11Å
$V_{P>11Å}$ – volume of pores with an average diameter of more than 11Å
W_s – porosity according to molecular probe analysis (benzene adsorption) method

Table 4. Comparison of capacitance (F cm^{-3}) values of the EDLC calculated per electrode pair volume, using different testing methods.

Capacitor #	ρ $[g\ cm^{-3}]$	Measurements procedure for capacitance [F cm^{-3}]		
		CV (10 mV s^{-1})	CC (10 mA)	EIS* (10 mHz)
SC 1	0.728	21.8	21.8	22.2
***SC* 2**	**0.707**	**22.1**	**22.3**	**23.0**
SC 3	0.643	17.8	18.5	18.9
SC 4	0.747	20.9	20.5	20.8
SC 5	0.703	23.1	22.7	23.0
SC 6	0.62	13.6	12.6	12.6

Capacitor # – test cell composed of respective carbon materials in Table 2 and Table 3
ρ – electrode material density
CV – cyclic voltammetry data
CC – constant current data
EIS* – electrochemical impedance data

Based on the data in Table 4 it was concluded that specific capacitance (F cm^{-3}) of novel carbide-derived carbon materials is in a high level compared to the activated carbon (sample 6). It is also interesting to note that *in situ* oxidation of carbon at certain conditions (sample 2), produces the similar electrochemical properties of the electrode compared to the specifically post-oxidized carbon (sample 5). This observation, however, is well supported by the similar porosity related parameters of the respective carbon material samples tested.

4.1 The cyclic voltammetry study

The cyclic voltammetry curves were recorded in the cell voltage range ΔU from 0 to 2.5V using a potential sweep-rate $5 < v < 50$ mV s^{-1}) according to $v = \pm dU/dt$[28,34,35]. The results are presented in Figs. 14 and 15. It was established that EDLCs are ideally polarizable in the applied voltage region [III-IV].

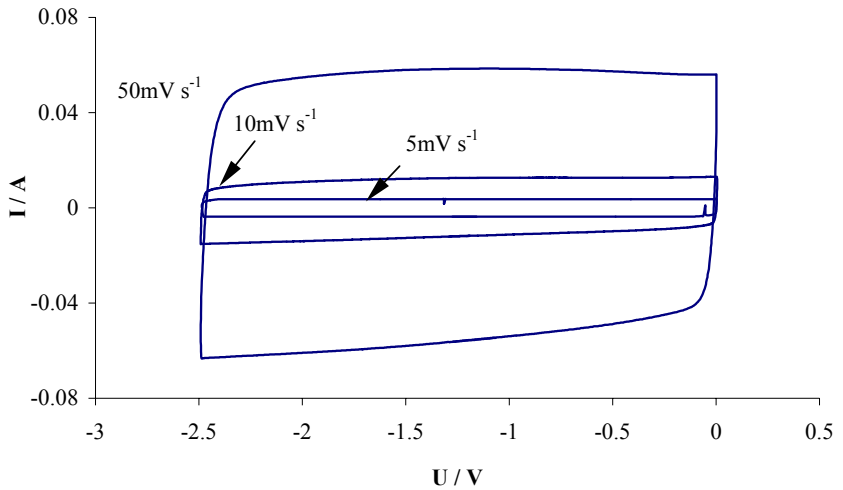

Figure 14. Cyclic voltammogram for "1 Farad" test-cell (SC 5) at different scan rates.

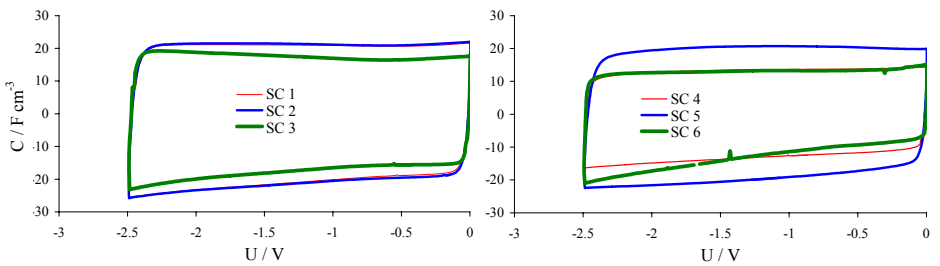

Figure 15. Cyclic voltammograms expressed as capacitance vs. voltage for different test cells (SC 1–6) at voltage scan rate 50mV s^{-1}. Capacitance is calculated per electrode pair volume.

In Fig. 14, it is seen that the current response of SC 5 only slightly increases with higher scan rate values. The voltammograms become distorted from the ideal rectangular shape characteristic for an ideal capacitor demonstrating the constant capacitance only at $v > 50$ mV s^{-1} [1].

Cyclic voltammograms expressed as capacitance vs. voltage are shown in Fig. 15. It is seen, that the capacitors based on the carbide-derived carbon

behave as almost ideal EDLC at a potential scan rate equal to or lower than 50 mV s^{-1}. The increased capacitance at higher voltage is caused by reduced effective size of the electrolyte ions absorbed due to the dependence of Gouy length on the surface charge density [33,34].

4.2 Constant Power Study

The energy versus power density relationship of the capacitors under study was derived from the so called Constant Power (CP) curves, recorded at room temperature in the voltage interval from 2.5V to 1.25V [III-V]. The results established are summarised as the Ragone plots in Fig. 16, where the energy and power densities are calculated per volume of the electrode pair and the timeframes 100-sec, 10-sec and 1-sec, noted in Figure 16, indicate the application times of supercapacitors [12,32,35].

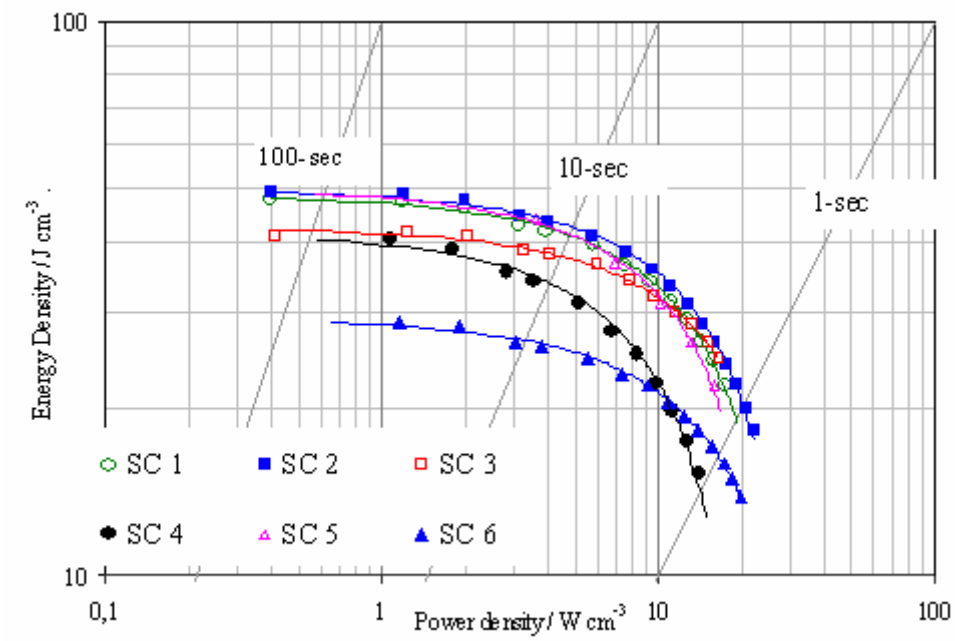

Figure 16. Ragone plot for supercapacitor cells during discharging from 2.5V to 1.25V at room temperature. The energy and power densities are calculated per volume of the electrode pair.

The volumetric energy densities at moderately low power density are rather similar for all SkeletonC supercapacitors tested. The capacitor SC 6 with conventional activated carbon electrodes possesses the lowest energy density, due to the lower bulk density of carbon, caused particularly by the larger size of the

micropores inside the material. The SC 3 and SC 4 are slightly different from the other SkeletonC capacitors [35], because the SC 3 capacitor cell was composed of microporous carbon with a relatively low density and with the highest specific surface area. Significant energy density decrease at higher power density values was observed for SC 4, where the most microporous carbon has been used. Comparison of data for supercapacitors SC 4 and SC 5 confirms significant positive effect of specific oxidation of carbon micropores to increase the power performance of respective supercapacitor [II–IV].

Table 5. Power density of SC cells per electrode pair volume at different application times.

Capacitor	Power density [W cm^{-3}]				
	18-sec	10-sec	5-sec	2-sec	1-sec
SC 1	2.5	4.2	7.4	13.7	19.2
SC 2	2.6	4.3	7.6	14.3	20.4
SC 3	2.3	3.8	7.0	13.8	20.5
SC 4	2.1	3.4	5.9	10.5	14.5
SC 5	2.5	4.2	7.2	13.1	17.9
SC 6	1.6	2.6	5.0	10.5	17.0

All capacitors based on carbon prepared from TiC/TiO_2 origin, have moderately high energy density and power performance at the short application time (i.e. below 10-sec). The power characteristics at different application times of supercapacitor cells are given in Table 5. The conventional carbon capacitor has the lowest volumetric power in the whole scale of applications. The capacitors based on the carbide-derived carbon, show similar power characteristics in applications exceeding the 10 seconds time limit. The shorter is the application time, the clearer is the advantage of TiC/TiO_2 based carbon materials.

4.3 Electrochemical impedance study

Electrochemical impedance spectroscopy data analysis is based on the *Z'',Z'* relationship data whereby jZ'' is the imaginary part of the impedance and Z' is frequency dependent ohmic resistance. Mathematically Z' and Z'' are connected according to the equation:

$$Z = Z' + Z'' = R + 1/\mathrm{j}\omega C \tag{9}$$

from which resistance *R* and capacitance *C* can be determined by frequency-response analysis in well-known ways [1, 36].

Z'',Z' or so called Nyquist plots presented in Figure 17 confirm that all EDLC test-cells of this study behave as typical capacitors over the frequency range from 100 Hz to 10 mHz.

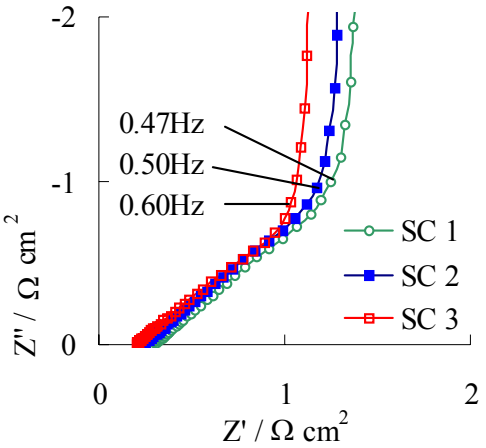

(a)

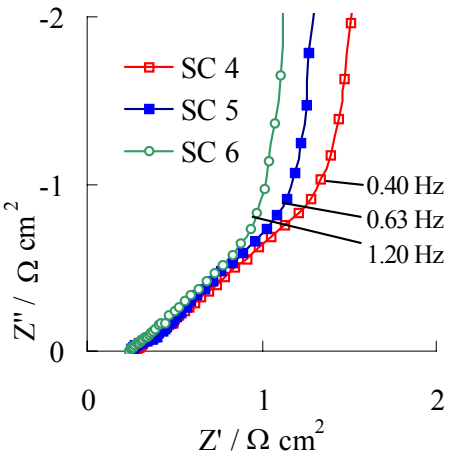

b)

Figure 17. Nyquist plots for different SC at ΔU=2.5V. SkeletonC materials of TiC/TiO_2 origins (a) and comparative carbon materials with different porosity (b).

The length and characteristics of the plateau in Z",Z'-plots with the ~45° slope in Figure 17 depend on many factors including electrode thickness, carbon porosity and density, separator and electrolyte characteristics, temperature and etc. The EDLC cells of this study differed from each other only by the carbon material characteristics. Therefore, the minor differences observed in this region of Nyquist plots are mainly caused by the different properties of the carbon

electrode and may particularly be contributed to the electrode material density. In the region of high-frequency ac, the porous electrode behaves like a planar surface and therefore the capacitance obtained is by many orders of magnitude lower compared to the equilibrium capacitance at $\omega \rightarrow 0$. This region of *Z''*,*Z'*-plots (usually at $f = 100$ Hz) is used to determine the series resistance of the electrical double-layer capacitor, $Z'_{(\omega \rightarrow 0)} = R_{\text{int.}}$.

Table 6. Different resistance values (Ω cm^2) and RC-constants for the EDLC calculated per electrode pair, using EIS testing method.

Capacitor	$R_{electrolyte}$	R_{1kHz}	RC
SC 1	0.291	0.323	0.75
SC 2	0.239	0.264	0.63
SC 3	0.202	0.220	0.43
SC 4	0.284	0.323	0.50
SC 5	0.252	0.294	0.77
SC 6	0.261	0.278	0.37

The resistance of dry carbon electrodes ($R_{electrode}$) investigated in this work is 0.035–0.045 Ω cm^2 as measured between the opposite planes of the electrode. The separator resistance (R_{sep}) is derived according to the equation:

$$R_{sep} = \frac{h \cdot 100}{\alpha \cdot \chi} \tag{10}$$

where χ is conductivity of the electrolyte [S], α is porosity of separator [%] and h is thickness of separator [cm].

Based on the electrolyte conductivity (56mS), separator thickness (24μm) and separator porosity (55%) the R_{sep} value is approximately 0.078 $\Omega \cdot$ cm^2, which is of the same order of magnitude as the electrode resistance. Thus, both the electrode and separator resistance are important in the high frequency region of AC impedance, determining mainly the so-called series resistance of the EDLC [37].

SUMMARY

The main object of this study was to find the optimal synthesis parameters for the titanium carbide derived carbon production process and to evaluate the application of the resulting microporous carbon materials in electrical double layer capacitors. The work has been divided into two main sections:

1) Optmization of the titanuim carbide derived carbon production process
2) Application and electrochemical evaluation of above mentioned carbide derived carbon in EDLC devices

The first section is focused on the implementation of the process cycle that allows for a more cost effective and flexible microporous carbon production process. Different stages of the process cycle were researched, to reveal the relationships between synthesis parameters and the porosity related features of the CDC. In particular, the titanium carbide synthesis stage and the titanium carbide chlorination stage were focused on, as these stages hold the key aspects for producing superior microporous carbon. In the carbide synthesis stage a shift in crystalline stoichiometry of TiC was observed, in accordance with the variations in synthesis temperature and the molar ratio of the precursor mixture. In the carbide chlorination stage it was further observed how these shifts in crystalline stoichiometry influence the parameters of the resulting microporous carbon. Optimized parameters for producing microporous carbon from titanium carbide through the process cycle were established from the research.

In the second part of the study, several microporous carbon materials were electrochemically evaluated in electrical double layer capacitor cells to research the effects of different oxidizing post-modification treatment methods on the performance of the EDLC cells. Cyclic voltammetry, constant power and electrochemical impedance methods were employed. It was established from the cyclic voltammetry and constant power studies, that the volumetric energy densities at moderately low power density are rather similar for all titanium carbide derived carbon based supercapacitors tested. The capacitors based on the carbide-derived carbon show rather similar power characteristics in applications exceeding the 10 seconds time limit. But the shorter the application time becomes, the clearer is the advantage of the materials that have been modified by the oxidizing post-treatment methods. Especially the *in situ* oxidation step by TiO_2 in the chlorination stage of the microporous carbon production process has been found to be very useful.

REFERENCES

1. E. Conway, Electrochemical supercapacitors. Scientific Fundamentals and Technological Applications, Kluwer Academic Publishers/Plenum, New York, 1999.
2. J. Chmiola, G. Yushin, Y. Gogotsi, C. Portet, P. Simon, L. Taberna, Science 313 (2006) 1760.
3. J. Chmiola, G. Yushin, R.K. Dash, Y. Gogotsi, J Power Sources, 158 (2005) 765–772.
4. M. Jacob, U. Palmqvist. P.C.A. Alberius, T. Ekstrom, M. Nygren, S. Lidin, Solid State Sciences 5(1) (2003) 133–137.
5. E. Johansson, B, Hjörtvarsson, T. Ekstrom, M. Jacob, J Alloys Compd (2002) 330–332:670–675.
6. J. Leis, A. Perkson, M. Arulepp, M. Käärik, G. Svensson, Carbon 39 (2001) 2043–2048.
7. A. Perkson, J. Leis, M. Arulepp, M. Käärik, S. Urbonaite, G. Svensson, Carbon 41 (2003) 1729–1735.
8. Y. Maletin, N. Strizhakova, S. Kozachkov, A. Mironova, S. Podmogilny, V. Danilin, J. Kolotilova, Y.V. Izotov, J. Cederström, S. Gordeev, J. Kukushkina, V. Sokolov, A. Kravchik, A. Perkson, M. Arulepp, J. Leis, A supercapacitor and a method of manufacturing such a supercapacitor. WO 02/39468, 2002.
9. M. Jacob, U. Palmqvist, T. Ekstrom, A. Henning, Mat. Res. Soc. Symp, (2000) 593, 87.
10. IUPAC. Compendium of Chemical Terminology, Blackwell, 1997.
11. H. Marsh, F. Rodriguez-Reinoso, Activated carbon, Oxford: Elsevier 2006.
12. S. J. Gregg, K.S.W. Sing, Adsorption, surface area and porosity, Moscow: MIR, 1984.
13. M. Kruk , M. Jaroniec, Chem. Mater. 13(10) (2001) 3169–3183.
14. F. Rouquerol, J. Rouquerol, K. Sing, Adsorption by Powders and Porous Solids: Principles, Methodology and Applications, Academic Press, London, 1999.
15. J. Jagiello, M. Thommes, Carbon 42(7) (2004) 1227–1232.
16. K.S.W. Sing, D.H. Everett, R.A.W. Haul, L. Moscou, R.A. Pierotti,J. Rouquerol, T. Siemieniewska, Pure Appl. Chem. 57 (1985) 603.
17. F. Shultz, KSW Sing, J. Weitkamp, Handbook of porous solids, Weinheim: Wiley VCH Verlag GmbH, 2002.
18. E. P. Barret, L. S, Joyner, P.P. Halenda, J. Am. Chem. Soc. 73 (1951) 373.
19. B.D. Cullity, Elements of X-ray Diffraction, Addison Wesley Mass. 1978.
20. B. E. Warren, X-ray diffraction, 1969, Addison-Wesley, Reading MA/Dover, Mineola NY.
21. A.E. Kravchik, A.S. Osmakov, R.G. Avarbe, Zhurn Prik Kh 62 (1989) 2430–5.
22. E. Smorgonskaya, R. Kytt, A. Danishevskii, C. Jardin, R. Meaudre, O. Marty, S. Gordeev, A. Grechinskaya, Journal of Non-Crystaline Solids, 810 (2002) 299–302.
23. J. Leis, A. Perkson, M. Arulepp, P. Nigu, G. Svensson, Carbon 40 (2002) 1559–1564.
24. A. Perkson, J. Leis, M. Arulepp, M. Käärik, S. Urbonaite, G. Svensson, Carbon 41 (2002) 1729–35.
25. G. Salitra, A. Soffer, L. Eliad, Y. Cohen, D. Aurbach, J Electrochem Soc. 146 (2000) 2486.
26. A. Jänes, L. Permann, M. Arulepp, E. Lust, Electrochem. Comm. 6 (2004) 313–318.

27. G.O. Shipton , Improvements in and relating to mineral active carbons and to a process for their preparation. GB 971943, 1964.
28. R. N. Kyutt, E. A. Smorgonskaya, A. M. Danishevski, S.K. Gordeev, A.V. Grechinskaya, Phys. Solid State 41 (1999) 1359–1363.
29. Y. Gogotsi, A. Nikitin, H. Ye,W. Zhou, J.E. Fischer, B.Yi, H.C. Foley, M.W. Barsoum, Nature Materials 2 (2003) 591–594.
30. A. Jerome. Mixed reactant molecular screen fuel cell. US 2005/0058875, 2005.
31. H. Simgen, G. Heusser, G. Zuzel, Applied Radiation and Isotopes 61 (2004) 213–217.
32. A. Burke, J. Power Sources 91 (2000) 37–50.
33. E. Lust, G. Nurk, A. Jänes, M. Arulepp, L. Permann, P. Nigu, P. Möller, Condensed Matter Physics, 5 (2002**)** 307.
34. E. Lust, N. Nurk, A. Jänes, M. Arulepp**,** P. Nigu, P. Möller, S. Kallip, V. Sammel-selg. J. Solid State Electrochem. 7 (2003) 91.
35. M. Arulepp. L. Permann, J, Leis, A. Perkson, K. Rumma, A. Jänes, E. Lust, J. Power Sources 133 (2004) 320.
36. ZView for Windows (ver. 3.0a), Scribner Assoc. Inc, Southern Pines, NC 28387
37. K. Tõnurist, A. Jänes, T. Thomberg, H. Kurig, E. Lust, J. of Electrochem. Soc. 156(4) (2009) A334 - A342.

SUMMARY IN ESTONIAN

Karbiidne mikropoorne süsinik ja elektrilise kaksikkihi kondensaatorid

Käesoleva uurimustöö eesmärgiks oli leida optimaalsed parameetrid titaankarbiidist sünteesitava mikropoorse süsiniku tootmiseks ja uurida võimalusi mikropoorsete süsinikmaterjalide rakendamiseks elektrokeemilise kaksikkihi kondensaatoris. Töö on jaotatud kahte ossa:

1) Mikropoorse karbiidse süsiniku tootmisprotsesssi optimiseerimine
2) Mikropoorsete süsinikmaterjalide rakendamine elektrokeemilise kaksikkihi kondensaatorites.

Töö esimene osa keskendub karbiidse mikropoorse süsiniku ringprotsessilise tootmistsükli uurimisele ja rakendamisele, et võimalda tootmisprotsessi kulude vähendamist ja kõrvalsaaduste säästlikku taaskasutamist. Tootmistsükli eri staadiumite katsetamisel püüti välja selgitada erinevate sünteesiparameetrite omavahelisi sõltuvusi ja nende mõju sünteesitava mikropoorse süsiniku omadustele. Titaankarbiidi sünteesi ja titaankarbiidi kloreerimise staadiumid olid erilise tähelepanu all, kuna nende tootmisprotsessi staadiumitega seonduvad sünteesiparameetrid avaldavad karbiidse mikropoorse süsiniku omadustele kõige suuremat mõju. Karbiidisünteesi staadiumi uurmisel ilmnes titankarbiidi kristallstruktuuris stöhhiomeetriline nihkumine, mille ulatus oli kooskõlas sünteesisegu molaarse koostise muutumisega. Titaankarbiidi kloreerimise staadiumis ilmesid selged sõltuvused karbiidi kristallstruktuuri stöhhiomeetrilise nihke ja saadava mikropoorse süsiniku omaduste vahel. Uurimustöö tulemusena leiti optimaalsed parameetrid titaankarbiidist kloreerimise teel saadava mikropoorse süsiniku tootmiseks.

Töö teises osas võrreldi mitmete erinevate omadustega süsinikmaterjale elektrokeemilise kaksikkihi kondensaatori rakenduses, et selgitada välja oksüdeerivate järeltöötlemismeetodite mõju süsinikmaterjalide käitumisele EKKK süsteemis. Uurimustöös kasutati mikropoorsete süsinikmaterjalide omaduste hindamiseks tsüklilise voltamperomeetria, konstantse võimsusega tühjenemise ja elektrokeemilise impedantsspktromeetria meetodeid. Tsüklilise voltamperomeetria ja konstantse võimsusega tühjenemise ekperimentide tulemustele toetudes võib väita, et ruumalalised energiatihedused mõõdukalt madalate võimsustiheduste juures, on kõikide titaankarbiidist sünteesitud süsinikmaterjalidel põhinevate EKKK rakkude puhul sarnased. Karbiidsel mikropoorsel süsinikul põhinevate EKKK rakkude võimsuskarakteristikud on sarnased, juhul kui rakendusaeg jääb ülespoole 10 sekundi piiri. Mida lühemaks muutub rakendusaeg, seda selgemalt väljenduvad oksüdeerivate järeltöötlemismeetodite abil modifitseeritud süsinikmaterjalide eelised. Eriti tugevalt ilmenvad lühikeste rakenduaegade puhul *in situ* TiO_2 abil kloreerimisfaasis modifitseeritud süsinikmaterjalide eelised.

ACKNOWLEDGEMENTS

I would like to thank my mentors professor Dr. Enn Lust and Dr. Alar Jänes who have guided me through many long years to this three letter goal. Very special thanks go to my colleagues Mati Arulepp and Jaan Leis, without your invaluable comments and contributions this goal would have been impossible to achieve. Special thanks go to the great synthesis team- Helle Kuura and Maike Käärik. Many thanks to Andres Kuura and Liina Permann for their help with the electrochemical experiments. Thanks to Rene Koka and Mare Riis for their help with the XRD and low temperature nitrogen sorption studies. I would also like to thank Kalle Loot, without the support of your technical knowledge and advice it would have been tough to keep the equipment running. I take a deep bow to all my colleagues at Carbon Nanotech OÜ and Tartu Tehnoloogiad OÜ.

I wish to thank my family and friends for their undivided love and support during all these years. Many thanks go to all the people who feel that they have contributed to this noble cause.

Tartu Tehnoloogiad OÜ and Carbon Nanotech OÜ are acknowledged for their financial support.

PUBLICATIONS

CURRICULUM VITAE

Given name and surname:	Marko Lätt
Date and place of birth:	30.05.1980, Võru
Citizenchip:	Estonian
Address:	Institute of Chemistry University of Tartu 2 Jakobi St., Tartu 51014, Estonia
E-mail address:	marko.latt@ut.ee, marko.latt@ee.henkel.com

Education

2005–…	University of Tartu, *Ph.D.* student (physical and electrochemistry)
2002–2005	University of Tartu, *M.Sc.* in physical and electrochemistry
1998–2002	University of Tartu, *B.Sc.* in materials science
1996–1998	Võru Kreutzwald high school

Professional employment

2009–….	Henkel Balti Ltd, R&D specialist
2001–2009	Tartu Technologies Ltd, chemist-technologist
1999–2001	University of Tartu, Institute of physical chemistry, chemist

List of publications

1. Arulepp, M., Leis, J., Kuura, A., Lätt, M., Kuura, H., Permann, L., Miller, F., Rumma, K. Performance of supercapacitors based on carbide derived SkeletonC. Proceedings of 15th International Seminar on Double Layer Capacitors & Hybrid Energy Storage Devices, 05.12–07.12.2005, Deerfield Beach, Florida, USA. 2005, 249–260.
2. Leis, J., Arulepp, M., Kuura, A., Lätt, M., Lust, E. Electrical double-layer characteristics of novel carbide-derived carbon materials. Carbon 2006, 44, 2122–2129
3. Arulepp, M., Leis, J., Lätt, M., Miller, F., Rumma, K., Lust, E., Burke, A.F. The advanced carbide-derived carbon based supercapacitor. J Power Sources 2006, 162, 1460–1466
4. Permann, L., Lätt, M., Leis, J., Arulepp, M. Electrical double layer characteristics of nanoporous carbon derived from titanium carbide. Electrochim. Acta 2006, 51, 1274–1281.

5. Lätt, M., Käärik, M., Permann, L., Kuura, H., Arulepp, M., Leis, J. A structural influence on the electrical double-layer characteristics of Al4C3-derived carbon. J Sol State Electrochem. 2008, doi:10.1007/s10008-008-0659-3

Patent applications:

1. "Method for manufacturing the nanoporous SkeletonC material", United States Patent Application No. US 0251565 A1.

Inventors: Jaan Leis, Mati Arulepp, Marko Lätt, Helle Kuura, Andres Kuura.

2. "Method of making the porous carbon material and porous carbon materials produced by the method", United States Patent Application No. 0117094 A1.

Inventors: Jaan Leis, Mati Arulepp, Marko Lätt, Helle Kuura.

3. "A method of making the composite carbon material with modified micro-structure and composite carbon materials produced by the method." Estonian patent application No. P200800008.

Inventors: Jaan Leis, Mati Arulepp, Marko Lätt, Helle Kuura, Andres Kuura.

ELULOOKIRJELDUS

Ees-ja perekonnanimi:	Marko Lätt
Sünniaeg ja koht:	30.05.1980, Võru
Kodakondsus:	Eesti
Aadress:	Keemia Instituut Tartu Ülikool Jakobi 2, Tartu 51014, Eesti
E-mail:	marko.latt@ut.ee, marko.latt@ee.henkel.com

Haridus

2005–…	Tartu Ülikool, Loodus- ja tehnoloogiadeaduskond, doktorant füüsikalise ja elektrokeemia erialal
2002–2005	Tartu Ülikool, Füüsika-keemiateaduskond, *M.Sc.* füüsikalise ja elektrokeemia erialal
1998–2002	Tartu Ülikool, Füüsika-keemiateaduskond, *B.Sc.* Materjaliteaduse erialal
1996–1998	Võru Kreutzwaldi Gümnaasium

Teenistuskäik

2009–….	Henkel Balti OÜ, tehnoloog
2001–2009	Tartu Tehnoloogiad OÜ, keemik-tehnoloog
1999–2001	Tartu Ülikool, Füüsikalise Kemia Instituut, keemik

Ilmunud teaduspublikatsioonid

1. Arulepp, M., Leis, J., Kuura, A., Lätt, M., Kuura, H., Permann, L., Miller, F., Rumma, K. Performance of supercapacitors based on carbide derived SkeletonC. Proceedings of 15th International Seminar on Double Layer Capacitors & Hybrid Energy Storage Devices, 05.12–07.12.2005, Deerfield Beach, Florida, USA. 2005, 249–260.
2. Leis, J., Arulepp, M., Kuura, A., Lätt, M., Lust, E. Electrical double-layer characteristics of novel carbide-derived carbon materials. Carbon 2006, 44, 2122–2129
3. Arulepp, M., Leis, J., Lätt, M., Miller, F., Rumma, K., Lust, E., Burke, A.F. The advanced carbide-derived carbon based supercapacitor. J Power Sources 2006, 162, 1460–1466
4. Permann, L., Lätt, M., Leis, J., Arulepp, M. Electrical double layer characteristics of nanoporous carbon derived from titanium carbide. Electrochim. Acta 2006, 51, 1274–1281.

5. Lätt, M., Käärik, M., Permann, L., Kuura, H., Arulepp, M., Leis, J. A structural influence on the electrical double-layer characteristics of Al4C3-derived carbon. J Sol State Electrochem. 2008, doi:10.1007/s10008-008-0659-3

Patenditaotlused

1. "Method for manufacturing the nanoporous SkeletonC material", United States Patent Application No. US 0251565 A1.

Inventors: Jaan Leis, Mati Arulepp, Marko Lätt, Helle Kuura, Andres Kuura.

2. "Method of making the porous carbon material and porous carbon materials produced by the method", United States Patent Application No. US 0117094 A1.

Inventors: Jaan Leis, Mati Arulepp, Marko Lätt, Helle Kuura.

3. "A method of making the composite carbon material with modified micro-structure and composite carbon materials produced by the method." Estonian patent application No. P200800008.

Inventors: Jaan Leis, Mati Arulepp, Marko Lätt, Helle Kuura, Andres Kuura.

DISSERTATIONES CHIMICAE UNIVERSITATIS TARTUENSIS

1. **Toomas Tamm.** Quantum-chemical simulation of solvent effects. Tartu, 1993, 110 p.
2. **Peeter Burk.** Theoretical study of gas-phase acid-base equilibria. Tartu, 1994, 96 p.
3. **Victor Lobanov.** Quantitative structure-property relationships in large descriptor spaces. Tartu, 1995, 135 p.
4. **Vahur Mäemets.** The ^{17}O and ^{1}H nuclear magnetic resonance study of H_2O in individual solvents and its charged clusters in aqueous solutions of electrolytes. Tartu, 1997, 140 p.
5. **Andrus Metsala.** Microcanonical rate constant in nonequilibrium distribution of vibrational energy and in restricted intramolecular vibrational energy redistribution on the basis of slater's theory of unimolecular reactions. Tartu, 1997, 150 p.
6. **Uko Maran.** Quantum-mechanical study of potential energy surfaces in different environments. Tartu, 1997, 137 p.
7. **Alar Jänes.** Adsorption of organic compounds on antimony, bismuth and cadmium electrodes. Tartu, 1998, 219 p.
8. **Kaido Tammeveski.** Oxygen electroreduction on thin platinum films and the electrochemical detection of superoxide anion. Tartu, 1998, 139 p.
9. **Ivo Leito.** Studies of Brønsted acid-base equilibria in water and non-aqueous media. Tartu, 1998, 101 p.
10. **Jaan Leis.** Conformational dynamics and equilibria in amides. Tartu, 1998, 131 p.
11. **Toonika Rinken.** The modelling of amperometric biosensors based on oxidoreductases. Tartu, 2000, 108 p.
12. **Dmitri Panov.** Partially solvated Grignard reagents. Tartu, 2000, 64 p.
13. **Kaja Orupõld.** Treatment and analysis of phenolic wastewater with microorganisms. Tartu, 2000, 123 p.
14. **Jüri Ivask.** Ion Chromatographic determination of major anions and cations in polar ice core. Tartu, 2000, 85 p.
15. **Lauri Vares.** Stereoselective Synthesis of Tetrahydrofuran and Tetrahydropyran Derivatives by Use of Asymmetric Horner-Wadsworth-Emmons and Ring Closure Reactions. Tartu, 2000, 184 p.
16. **Martin Lepiku.** Kinetic aspects of dopamine D_2 receptor interactions with specific ligands. Tartu, 2000, 81 p.
17. **Katrin Sak.** Some aspects of ligand specificity of P2Y receptors. Tartu, 2000, 106 p.
18. **Vello Pällin.** The role of solvation in the formation of iotsitch complexes. Tartu, 2001, 95 p.

19. **Katrin Kollist.** Interactions between polycyclic aromatic compounds and humic substances. Tartu, 2001, 93 p.
20. **Ivar Koppel.** Quantum chemical study of acidity of strong and superstrong Brønsted acids. Tartu, 2001, 104 p.
21. **Viljar Pihl.** The study of the substituent and solvent effects on the acidity of OH and CH acids. Tartu, 2001, 132 p.
22. **Natalia Palm.** Specification of the minimum, sufficient and significant set of descriptors for general description of solvent effects. Tartu, 2001, 134 p.
23. **Sulev Sild.** QSPR/QSAR approaches for complex molecular systems. Tartu, 2001, 134 p.
24. **Ruslan Petrukhin.** Industrial applications of the quantitative structure-property relationships. Tartu, 2001, 162 p.
25. **Boris V. Rogovoy.** Synthesis of (benzotriazolyl)carboximidamides and their application in relations with *N*- and *S*-nucleophyles. Tartu, 2002, 84 p.
26. **Koit Herodes.** Solvent effects on UV-vis absorption spectra of some solvatochromic substances in binary solvent mixtures: the preferential solvation model. Tartu, 2002, 102 p.
27. **Anti Perkson.** Synthesis and characterisation of nanostructured carbon. Tartu, 2002, 152 p.
28. **Ivari Kaljurand.** Self-consistent acidity scales of neutral and cationic Brønsted acids in acetonitrile and tetrahydrofuran. Tartu, 2003, 108 p.
29. **Karmen Lust.** Adsorption of anions on bismuth single crystal electrodes. Tartu, 2003, 128 p.
30. **Mare Piirsalu.** Substituent, temperature and solvent effects on the alkaline hydrolysis of substituted phenyl and alkyl esters of benzoic acid. Tartu, 2003, 156 p.
31. **Meeri Sassian.** Reactions of partially solvated Grignard reagents. Tartu, 2003, 78 p.
32. **Tarmo Tamm.** Quantum chemical modelling of polypyrrole. Tartu, 2003. 100 p.
33. **Erik Teinemaa.** The environmental fate of the particulate matter and organic pollutants from an oil shale power plant. Tartu, 2003. 102 p.
34. **Jaana Tammiku-Taul.** Quantum chemical study of the properties of Grignard reagents. Tartu, 2003. 120 p.
35. **Andre Lomaka.** Biomedical applications of predictive computational chemistry. Tartu, 2003. 132 p.
36. **Kostyantyn Kirichenko.** Benzotriazole — Mediated Carbon–Carbon Bond Formation. Tartu, 2003. 132 p.
37. **Gunnar Nurk.** Adsorption kinetics of some organic compounds on bismuth single crystal electrodes. Tartu, 2003, 170 p.
38. **Mati Arulepp.** Electrochemical characteristics of porous carbon materials and electrical double layer capacitors. Tartu, 2003, 196 p.
39. **Dan Cornel Fara.** QSPR modeling of complexation and distribution of organic compounds. Tartu, 2004, 126 p.

40. **Riina Mahlapuu.** Signalling of galanin and amyloid precursor protein through adenylate cyclase. Tartu, 2004, 124 p.
41. **Mihkel Kerikmäe.** Some luminescent materials for dosimetric applications and physical research. Tartu, 2004, 143 p.
42. **Jaanus Kruusma.** Determination of some important trace metal ions in human blood. Tartu, 2004, 115 p.
43. **Urmas Johanson.** Investigations of the electrochemical properties of polypyrrole modified electrodes. Tartu, 2004, 91 p.
44. **Kaido Sillar.** Computational study of the acid sites in zeolite ZSM-5. Tartu, 2004, 80 p.
45. **Aldo Oras.** Kinetic aspects of dATPαS interaction with $P2Y_1$ receptor. Tartu, 2004, 75 p.
46. **Erik Mölder.** Measurement of the oxygen mass transfer through the air-water interface. Tartu, 2005, 73 p.
47. **Thomas Thomberg.** The kinetics of electroreduction of peroxodisulfate anion on cadmium (0001) single crystal electrode. Tartu, 2005, 95 p.
48. **Olavi Loog.** Aspects of condensations of carbonyl compounds and their imine analogues. Tartu, 2005, 83 p.
49. **Siim Salmar.** Effect of ultrasound on ester hydrolysis in aqueous ethanol. Tartu, 2006, 73 p.
50. **Ain Uustare.** Modulation of signal transduction of heptahelical receptors by other receptors and G proteins. Tartu, 2006, 121 p.
51. **Sergei Yurchenko.** Determination of some carcinogenic contaminants in food. Tartu, 2006, 143 p.
52. **Kaido Tämm.** QSPR modeling of some properties of organic compounds. Tartu, 2006, 67 p.
53. **Olga Tšubrik.** New methods in the synthesis of multisubstituted hydrazines. Tartu. 2006, 183 p.
54. **Lilli Sooväli.** Spectrophotometric measurements and their uncertainty in chemical analysis and dissociation constant measurements. Tartu, 2006, 125 p.
55. **Eve Koort.** Uncertainty estimation of potentiometrically measured ph and pK_a values. Tartu, 2006, 139 p.
56. **Sergei Kopanchuk.** Regulation of ligand binding to melanocortin receptor subtypes. Tartu, 2006, 119 p.
57. **Silvar Kallip.** Surface structure of some bismuth and antimony single crystal electrodes. Tartu, 2006, 107 p.
58. **Kristjan Saal.** Surface silanization and its application in biomolecule coupling. Tartu, 2006, 77 p.
59. **Tanel Tätte.** High viscosity $Sn(OBu)_4$ oligomeric concentrates and their applications in technology. Tartu, 2006, 91 p.
60. **Dimitar Atanasov Dobchev**. Robust QSAR methods for the prediction of properties from molecular structure. Tartu, 2006, 118 p.

61. **Hannes Hagu**. Impact of ultrasound on hydrophobic interactions in solutions. Tartu, 2007, 81 p.
62. **Rutha Jäger.** Electroreduction of peroxodisulfate anion on bismuth electrodes. Tartu, 2007, 142 p.
63. **Kaido Viht.** Immobilizable bisubstrate-analogue inhibitors of basophilic protein kinases: development and application in biosensors. Tartu, 2007, 88 p.
64. **Eva-Ingrid Rõõm.** Acid-base equilibria in nonpolar media. Tartu, 2007, 156 p.
65. **Sven Tamp.** DFT study of the cesium cation containing complexes relevant to the cesium cation binding by the humic acids. Tartu, 2007, 102 p.
66. **Jaak Nerut.** Electroreduction of hexacyanoferrate(III) anion on Cadmium (0001) single crystal electrode. Tartu, 2007, 180 p.
67. **Lauri Jalukse.** Measurement uncertainty estimation in amperometric dissolved oxygen concentration measurement. Tartu, 2007, 112 p.
68. **Aime Lust.** Charge state of dopants and ordered clusters formation in CaF_2:Mn and CaF_2:Eu luminophors. Tartu, 2007, 100 p.
69. **Iiris Kahn**. Quantitative Structure-Activity Relationships of environmentally relevant properties. Tartu, 2007, 98 p.
70. **Mari Reinik.** Nitrates, nitrites, N-nitrosamines and polycyclic aromatic hydrocarbons in food: analytical methods, occurrence and dietary intake. Tartu, 2007, 172 p.
71. **Heili Kasuk.** Thermodynamic parameters and adsorption kinetics of organic compounds forming the compact adsorption layer at Bi single crystal electrodes. Tartu, 2007, 212 p.
72. **Erki Enkvist.** Synthesis of adenosine-peptide conjugates for biological applications. Tartu, 2007, 114 p.
73. **Svetoslav Hristov Slavov**. Biomedical applications of the QSAR approach. Tartu, 2007, 146 p.
74. **Eneli Härk.** Electroreduction of complex cations on electrochemically polished Bi(*hkl*) single crystal electrodes. Tartu, 2008, 158 p.
75. **Priit Möller.** Electrochemical characteristics of some cathodes for medium temperature solid oxide fuel cells, synthesized by solid state reaction technique. Tartu, 2008, 90 p.
76. **Signe Viggor.** Impact of biochemical parameters of genetically different pseudomonads at the degradation of phenolic compounds. Tartu, 2008, 122 p.
77. **Ave Sarapuu.** Electrochemical reduction of oxygen on quinone-modified carbon electrodes and on thin films of platinum and gold. Tartu, 2008, 134 p.
78. **Agnes Kütt.** Studies of acid-base equilibria in non-aqueous media. Tartu, 2008, 198 p.
79. **Rouvim Kadis.** Evaluation of measurement uncertainty in analytical chemistry: related concepts and some points of misinterpretation. Tartu, 2008, 118 p.

80. **Valter Reedo.** Elaboration of IVB group metal oxide structures and their possible applications. Tartu, 2008, 98 p.
81. **Aleksei Kuznetsov.** Allosteric effects in reactions catalyzed by the cAMP-dependent protein kinase catalytic subunit. Tartu, 2009, 133 p.
82. **Aleksei Bredihhin.** Use of mono- and polyanions in the synthesis of multisubstituted hydrazine derivatives. Tartu, 2009, 105 p.
83. **Anu Ploom.** Quantitative structure-reactivity analysis in organosilicon chemistry. Tartu, 2009, 99 p.
84. **Argo Vonk.** Determination of adenosine A_{2A}- and dopamine D_1 receptor-specific modulation of adenylate cyclase activity in rat striatum. Tartu, 2009, 129 p.
85. **Indrek Kivi.** Synthesis and electrochemical characterization of porous cathode materials for intermediate temperature solid oxide fuel cells. Tartu, 2009, 177 p.
86. **Jaanus Eskusson.** Synthesis and characterisation of diamond-like carbon thin films prepared by pulsed laser deposition method. Tartu, 2009, 117 p.